

Determining the Optimal Printing Conditions for the Production of a Fertigation Pump Prototype with FDM Technology

ALEXANDRU-POLIFRON CHIRITA*, GHEORGHE SOVAIALA, VALENTIN BARBU, MARIAN BLEJAN, IOAN PAVEL

INOE 2000-Subsidiary Hydraulics and Pneumatics Research Institute, 14 Cutitul de Argint Str., 040558, Bucharest, Romania

Abstract: *The article presents the optimization of a production process with the help of FDM technology of a fertigation pump prototype that does not require other energy source than that given by the flow and pressure of water for irrigation. In the research presented in this article specimens of PETG material are tested in terms of mechanical properties by using a tensile test equipment. The results of these tests are used to dimension and simulate with finite element the component elements of the pump.*

Keywords: *FDM, prototyping, PET-G, fertigation pump, finite element, tensile testing, specimens*

1. Introduction

3D printing (3DP), specifically fused deposition modeling (FDM), is one of the most accessible and widespread rapid prototyping technologies [1]. Recent advances in additive manufacturing (AM) - a construction technique where a three-dimensional object is created through the build-up of thin layers of a thermoplastic material - have resulted in the commercialization and popularization of what is commonly known as 3DP. Objects for 3D printing are stored in digital files for modification using 3D modeling software, and are easily copied and transferred via the Internet. Rapid prototyping procedures make it possible to produce relatively complicated parts based on computer 3D geometries. Most of the rapid prototyping processes can create parts from a variety of common and special materials [2, 3]. FDM technology was used for the production of the fertigation pump due to the speed with which the printed components can be iterated and due to the low production cost [4, 5].

Fertilization is the direct injection of fertilizer into the irrigation pipeline, using special pumping equipment. The fertigation equipment, developed to the prototype phase, is intended for the fertigation of horticultural crops practiced in arid, semi-arid and dry sub-humid climate conditions, working in aggregate with drip irrigation installations [6].

When making the primary solution injection device, that is the main component of the equipment and is presented in the article, innovative and original technical solutions for the fertigation field were used, regarding the materials used in the manufacturing process and the operating principle. The injection device (of differential piston type), presented in Figure 1, uses as working fluid the irrigation water taken from the main pipe of the irrigation plant (the same pipe in which the primary solution is injected), which ensures its autonomy of operation at any point of the irrigation facility. The injection pressure is made on the principle of the difference of the active surfaces of the drive piston and injection piston, established according to the hydraulic parameters of the irrigation plant from the device design phase. The flow of the injected primary substance can be adjusted within wide limits, by modifying the supply flow of the drive chambers, implicitly the frequency of the mobile assembly formed by the drive piston, the injection piston and the control mechanism of the control module [7].

The fertigation equipment will be mounted in parallel with the main circuit of the irrigation system (by-pass system) [8] through two quick couplings. The subject of the paper is the production of a prototype pump for fertigation with FDM technology and the objective is to determine the optimal printing conditions of the PETG filament so that it can withstand the mechanical stresses to which it is subjected.

*email: chirita.ihp@fluidas.ro

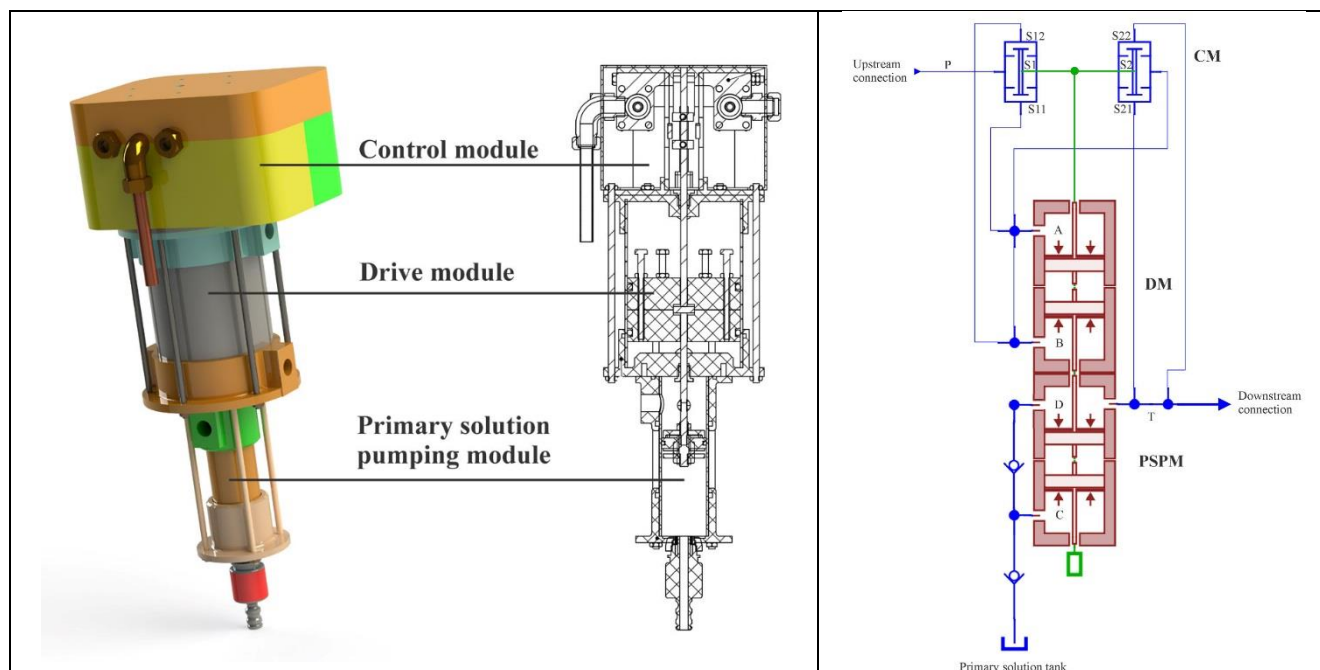


Figure 1. Prototype of the fertigation pump - 3D model, section view and functional diagram

2. Materials and methods

This chapter presents the equipment, means and process by which the prototype fertigation pump was produced.

2.1. Tensile testing of PETG specimens

For the experimental determination of the tensile strength, especially in the case of specimens printed on the Z (vertical) orientation, the double column test stand equipped with a force transducer and the displacement transducer was used, a picture of which is shown in Figure 2. It can measure a force of maximum 5000 N due to the measuring range of the transducer, which is smaller than what the stand can produce, the stroke is 300 mm and the speed can be varied in the range of 3.4-242 mm/min.

In addition, the shape and dimensions of the specimens are presented in Figure 2; they do not meet a specific standard but were inspired by the ASTM D638-14 [9]. The test speed was 6 mm/min.

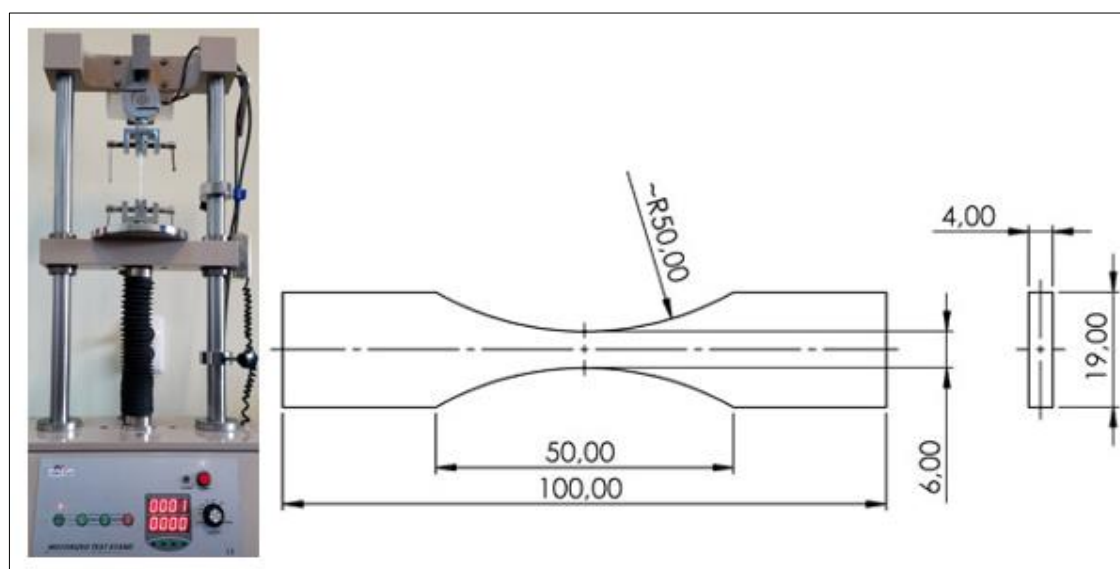


Figure 2. SAMA-SAHDV-10K double column test stand and specimen dimensions

This shape was chosen so that the specimens could be printed in both vertical (Z) and horizontal (XY) orientation. Figure 3 shows the dimensions measured for the specimens printed in the Z orientation; usually they have a lower dimensional accuracy than those printed in the XY orientation

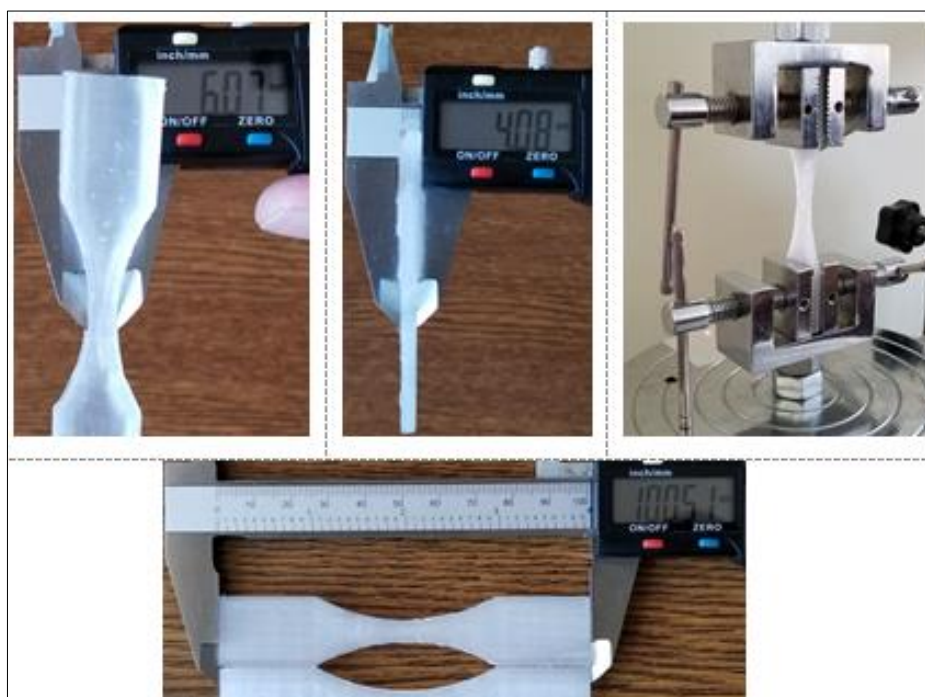


Figure 3. Dimensions of the specimens for tensile testing and their fixing in the universal jaws

Figure 4 shows the specimens from batch 4, during the printing process but also at the end of it. It can be seen that both orientations were printed simultaneously in the same humidity conditions of the material.

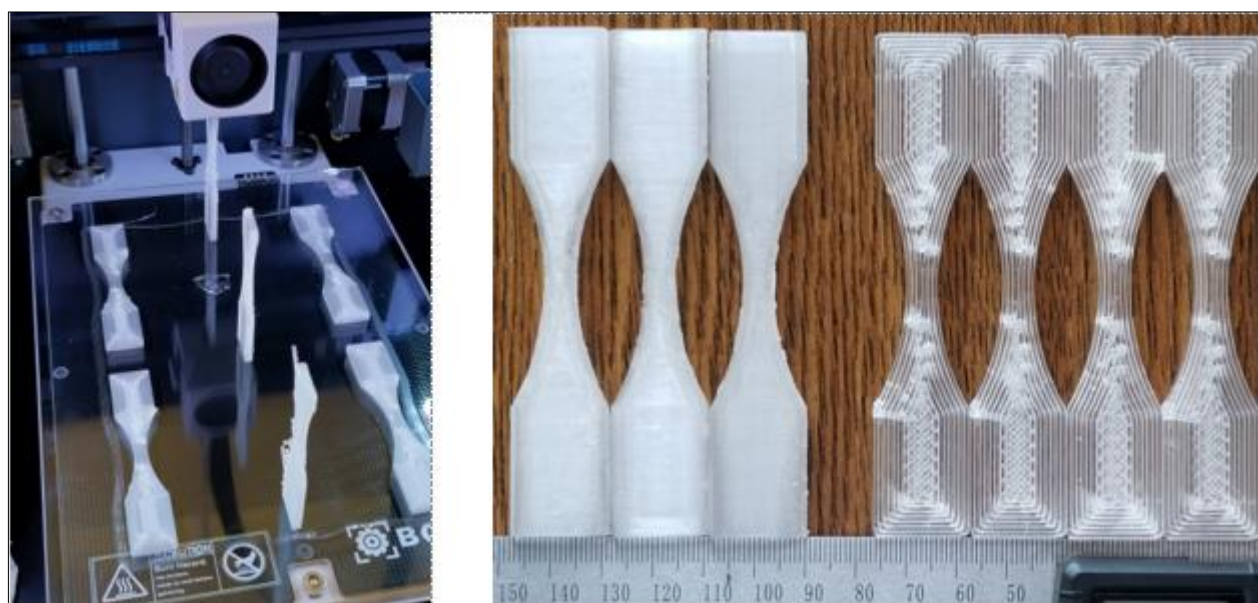


Figure 4. Specimens during and at the end of the printing process (batch 4)

The photos in the presented figures were taken with a camera, and the details of various degrees of magnification were taken with the KRUSS MBL2150 microscope, shown in Figure 5.

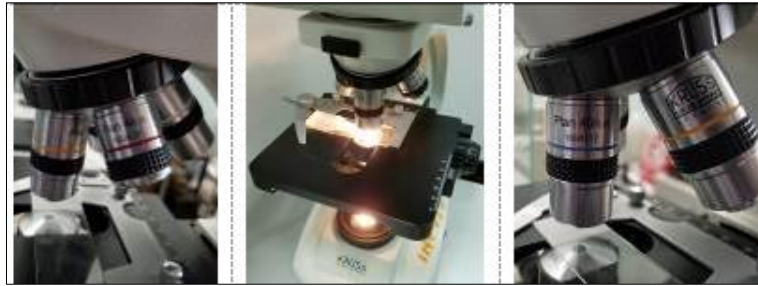


Figure 5. KRUSS MBL2150 microscope

2.2. Finite element numerical simulation of a pump component

The design and sizing of the pump components was performed with CAD / CAE SOLIDWORKS software, and in group of Figure 5 one can see one of them; on the left side the 3D model of the flange is presented, in the middle, in the green color, one can see its connections with the other components and on the right side, the surfaces on which the pressure of 6 bar acts are marked in blue.

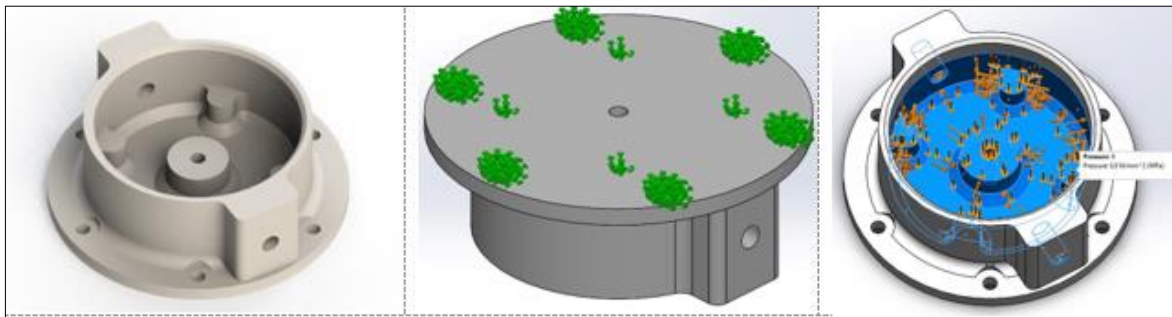


Figure 6. 3D model of the flange, fixed surfaces (green) and surfaces on which the pressure of 6 bar acts (blue)

Figure 7 shows the mesh and the new profile of the PETG material with which the finite element analyzes will be performed. Most of the parameters are from the filament product datasheet but the values for TS and YS are those determined experimentally for printing in the Z orientation.

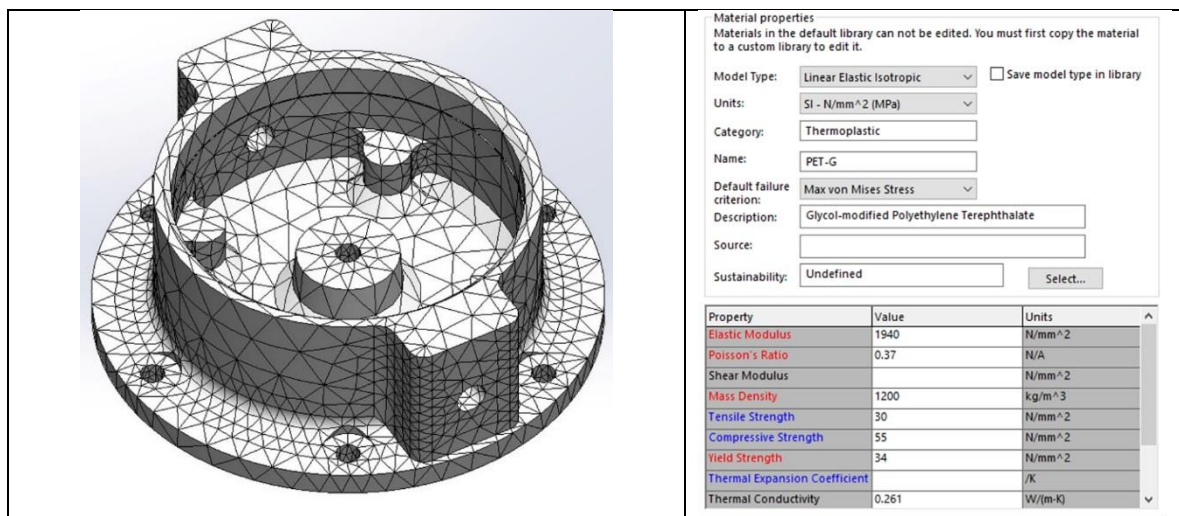


Figure 7. The size and quality of the mesh of the 3D model and the definition of the mechanical properties of the new material

2.3. The 3D printing process of the pump prototype components

Printing was done on the BCN3D SIGMA R19 printer with the following facilities:

- Architecture: Independent Dual Extruder (IDEX);
 - Printing volume: 210 mm x 297 mm x 210 mm;
 - Heated bed maximum temperature: 100°C;
 - Positioning resolution (X/Y/Z): 1.25 μ m/ 1.25 μ m/ 1 μ m;
 - Firmware: BCN3D Sigma - Marlin;
 - Extruder system Extruder Bondtech™ high-tech dual drive gears; Hotends: Optimized and manufactured by e3D™;
 - The hotend nozzle on the right is 1 mm in diameter;
 - File preparation software: BCN3D Cura, shown in Figure 7;
- The printer and a picture during the printing process are shown in Figure 8.

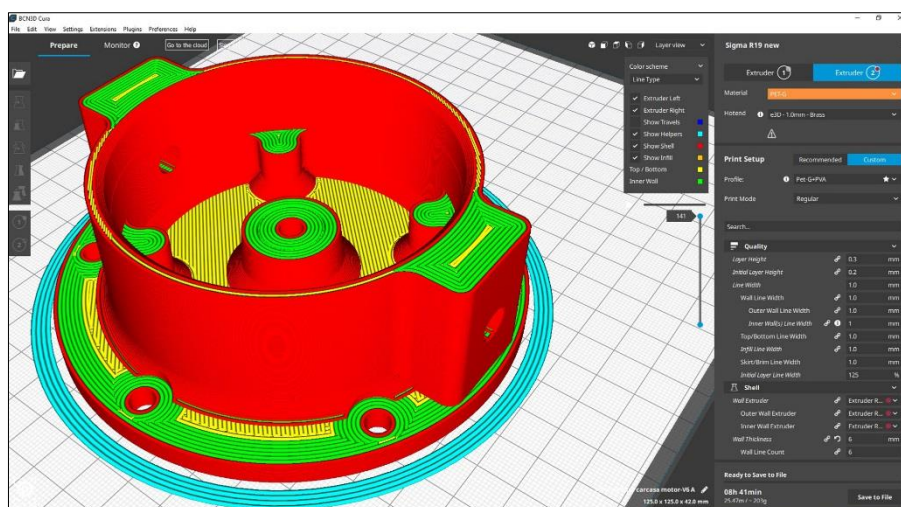


Figure 8. File preparation software - BCN3D Cura

All the parts of the prototype were printed with PETG filament and for the parts that needed support PVA was used, which dissolves easily in water.

Parameters of the 3D printing process: the filament diameter was 2.85 mm, nozzle with a diameter of 1 mm, 0.3 mm layer height, 35% or 100% infill density, 205°C printing temperature, 75°C build plate temperature and a conservative print speed of 20 mm/s.

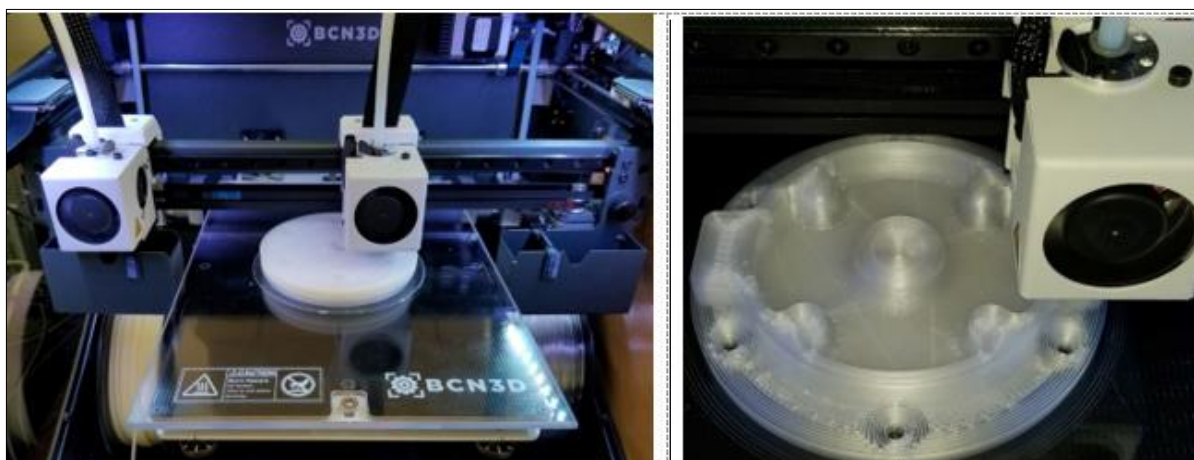


Figure 9. The BCN3D SIGMA R19 3D printer

3. Results and discussions

In this chapter, the following results are presented and centralized: tensile tests, finite element analysis and those of the 3D printing process.

3.1. Tensile testing results

Figure 10 shows the specimens printed in XY orientation after the tensile test as well as some details captured under a microscope, in which one can see that the material is ductile and the creep phenomenon occurs, and the layers tend to separate in the planes perpendicular to the longitudinal axis of the specimen.

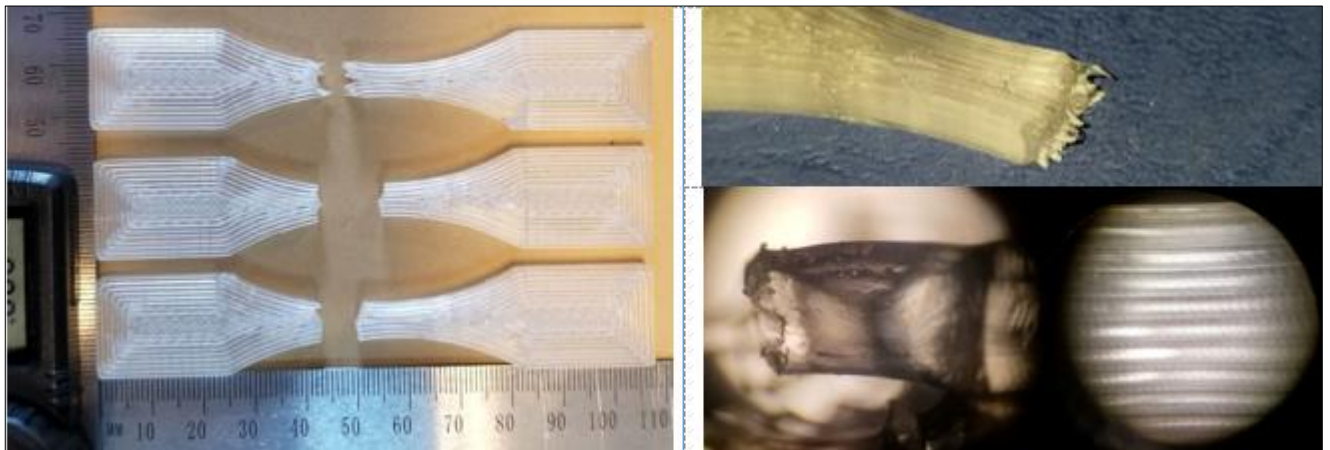


Figure 10. Specimens (XY printing orientation) after tensile testing and their details

The specimens in Figure 11 were printed in the Z orientation, and in the details of this figure one can see that the detachment of the two halves of the specimen did not occur at the intersection of only two layers, which means that the adhesion of the layers is very good. Also, in the details of this figure one can see that the layers no longer separate perpendicular to the longitudinal axis of the specimen, they tear each other, and another important aspect to mention is the effect of filament moisture; it penetrates with the filament in the extruder and when the filament is extruded creates a gas bubble that weakens the strength of the part.

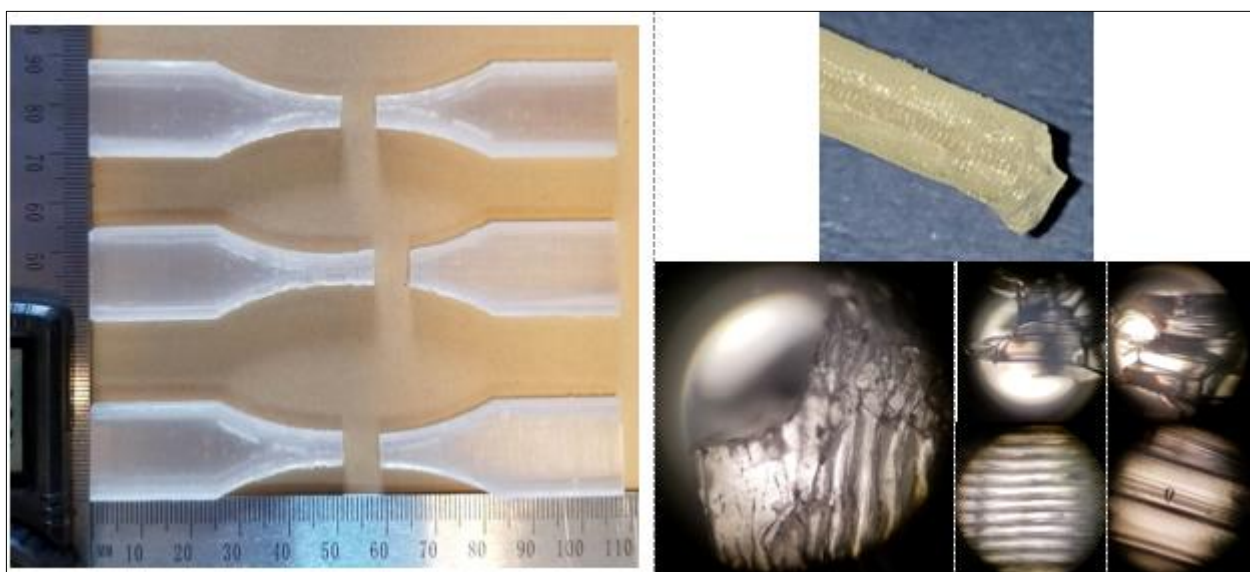


Figure 11. Specimens (Z printing orientation) after tensile testing and their details

Stress–strain curves are shown in Figure 12 for both printing orientations. One can see that unlike the Z orientation, XY resists a higher stress and the elongation is about three times greater. Similar results can be noticed in the specialized literature [10, 11].

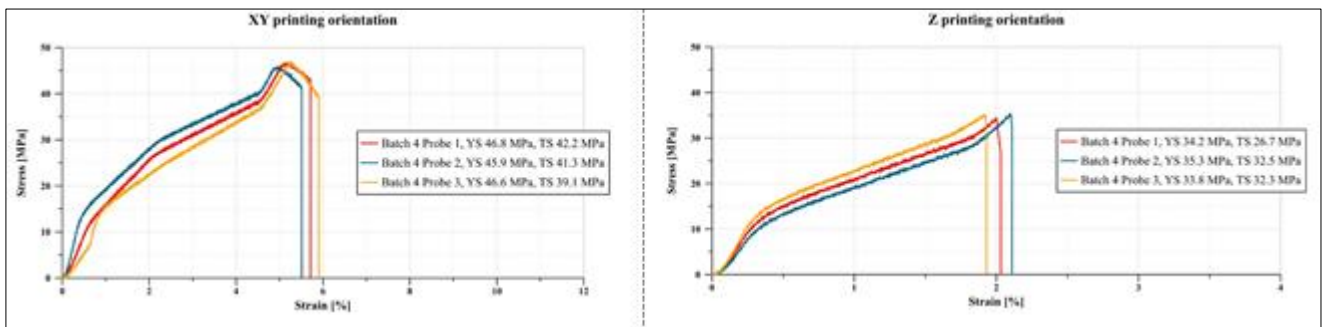


Figure 12. Stress–strain curves (batch 4)

The filament manufacturer recommends printing temperatures between 195 - 225 degrees Celsius and to determine the optimal printing temperature, batches 1, 2 and 3 were tested at different temperatures according to the graph in Figure 12. After testing with different temperatures, the one of 205 degrees Celsius was chosen as the optimal one; this makes a small compromise in terms of workpiece strength and printing speed but delivers good dimensional accuracy.

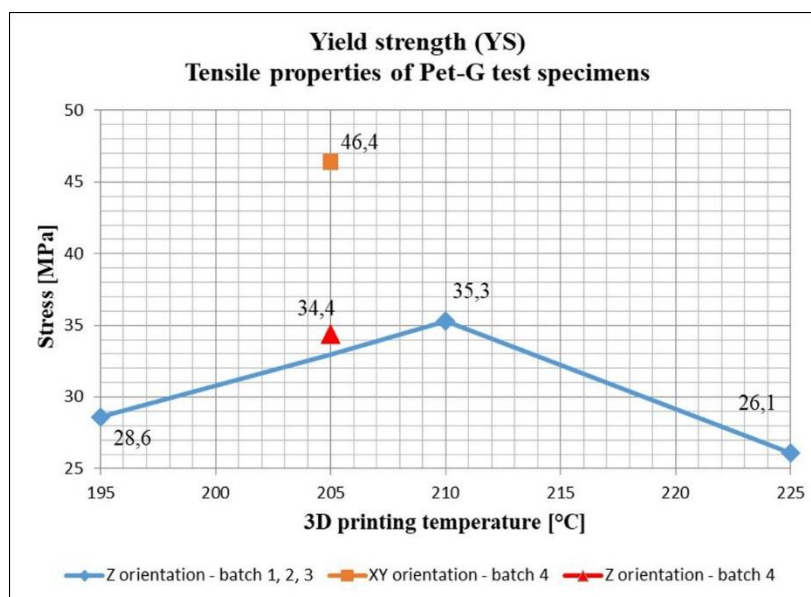


Figure 13. Centralizer of all tensile tests for different orientation of printed specimen and four printing temperatures

3.2. Finite element analysis results

Following the Von Mises analysis presented in Figure 13, the following can be highlighted: the maximum stress to which the part is subjected is 23.5 MPa, it withstands up to 34 MPa and only 0.10% of the geometric volume of the piece or 0.45% of the volume of the finished elements are subjected at demands higher than 15 MPa.

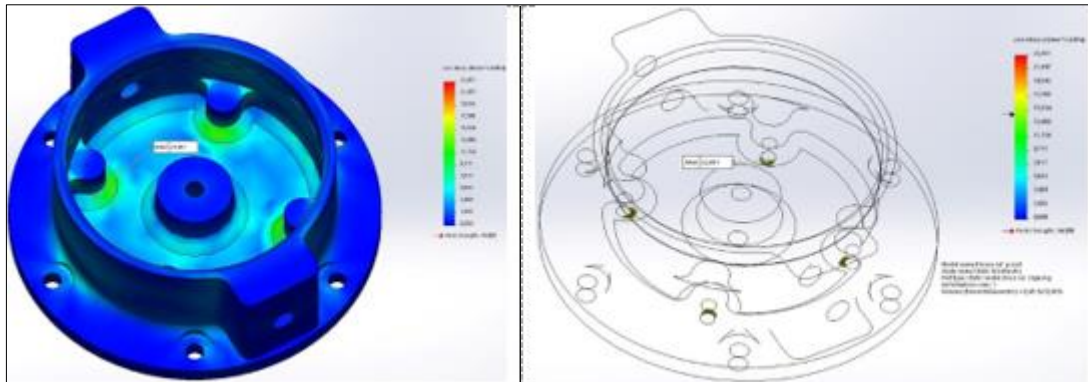


Figure 14. Von Mises stress analysis

Figure 14 shows the maximum deformation of the part caused by the pressure of 6 bar; it does not exceed 0.24 mm. The deformation in operation will never reach these values because the nominal working pressure is somewhere between 2 and 4 bar, and the pressure of 6 bar is the maximum pressure at which the system can operate for a short time. In the same figure, on the right side the diagram of the safety factor is presented, whose minimum value is 1.45.

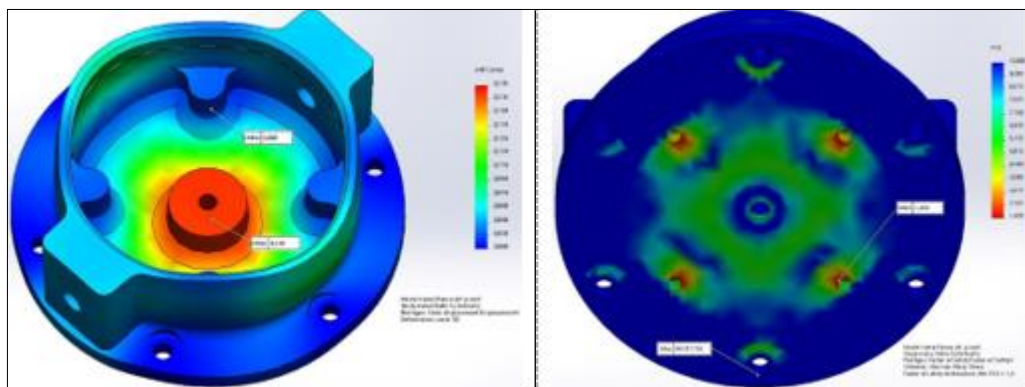


Figure 15. Deformation of the part and the diagram of the safety factor

3.3. The results of the 3D printing process



Figure 16. Almost all the 3D printed components of the fertigation pump

Figure 16 shows the results of the production process of the fertigation pump using FDM technology. These include caps, walls, valve bodies, bar mechanism, flanges, pistons, one-way valve, elastic TPU element, a spherical joint, and others. Because of space constraints in this paper, it was chosen to present

only the process of design, verification and manufacture of the flange, this being one of the components under the highest mechanical stress.

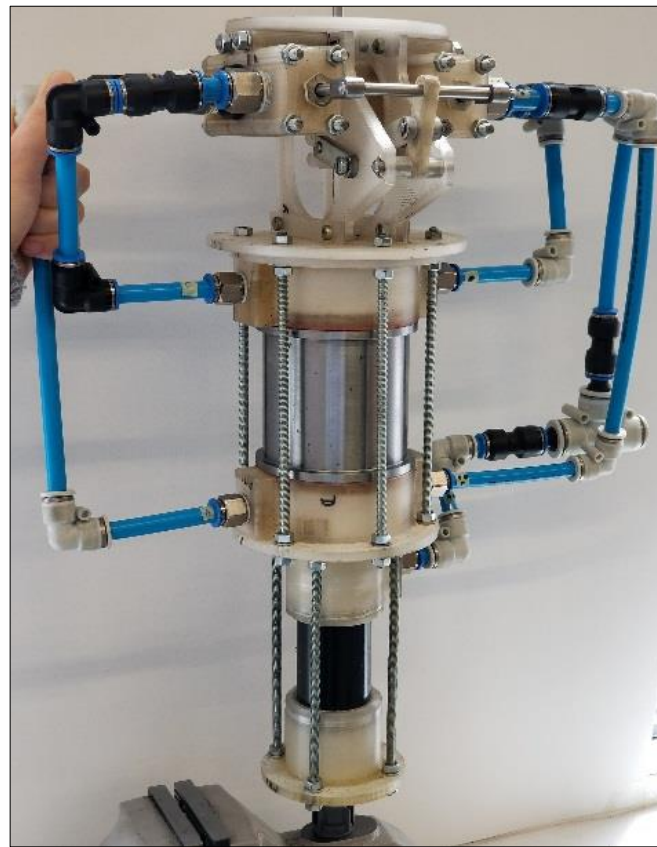


Figure 17. Fertigation pump prototype

Figure 17 presents the prototype of the fertigation pump between two functional tests.

4. Conclusions

Over 35 functional components of the fertigation pump have been produced with PETG material due to its resistance to corrosive liquids.

Almost 90% of the volume of the pump components were produced with FDM technology due to the possibility of faster iteration of the revised parts.

The printed elements of the pump weigh about 3 kg.

Results of tensile tests of 3D printed specimens are consistent with those in the specialized literature.

In a future article the design and sizing of another essential component of the pump produced with the same technology, namely the piston of the drive module, will be presented, as well as the experimental results in operation of this fertigation pump.

Acknowledgments: This paper has been funded by a grant of the Romanian Ministry of Research and Innovation under Programme I-Development of national R&D system, Subprogramme 1.2–Institutional performance–Projects financing excellence in R&D&I, Project acronym: PRO-INSTITUTIO, Financial Agreement no. 19PFE/17.10.2018, Phase 5, while the scientific results presented were obtained under Project INNOVATIVE TECHNOLOGIES FOR IRRIGATION OF AGRICULTURAL CROPS IN ARID, SEMIARID AND SUBHUMID-DRY CLIMATE, project number PN-III-P1-1.2-PCCDI-2017-0254, Contract no. 27PCCDI / 2018, within PNCDI III.



References

1. BORDONI, M., BOSCHETTO, A., Thickening of surfaces for direct additive manufacturing fabrication, *Rapid Prototyping J.*, **18** (4), 2012, 308-318.
2. ADAM, G., ZIMMER, D., On design for additive manufacturing: Evaluating geometrical limitations, *Rapid Prototyping J.*, **21** (6), 2015, 662-670.
3. NOVAKOVA-MARCININOVA, L., KURIC, I., Basic and advanced materials for fused deposition modeling rapid prototyping technology, *Manuf. and Ind. Eng.*, **11** (1), 2012, 24-27.
4. SURANGE, V. G., GHARAT, P. V., 3D Printing Process Using Fused Deposition Modelling (FDM), *International Research Journal of Engineering and Technology (IRJET)*, **3** (3), 2016, 1403-1406.
5. PETRICK, I. J., SIMPSON, T. W., 3D Printing Disrupts Manufacturing: How Economies of One Create New Rules of Competition, *Research-Technology Management*, **56** (6), 2015, 12-16.
6. BLIDARU, V., PRICOP, Gh., WEHRY, A., *Irigatii si drenaje / Irrigation and drainage*, Didactic and Pedagogical Publishing House, Bucharest, 1981, 258-278.
7. AVRAM, M., *Actionari hidraulice si pneumatice / Hydraulic and pneumatic drives*, University Publishing House, Bucharest, 2005, 172-190.
8. BIOLAN, I., SERBU, I., SOVAIALA, Gh., MARDARE, F., *Tehnici si tehnologii de fertirigare a culturilor agricole / Techniques and technologies for fertigation of agricultural crops*, AGIR Publishing House, 2010, 58-59.
9. *** Standard Test Method for Tensile Properties of Plastics - ASTM D638 – 14.
10. LATKO-DURALEK, P., DYDEK, K., BOCZKOWSKA, A., Thermal, Rheological and Mechanical Properties of PETG/rPETG Blends, *Journal of Polymers and the Environment*, **27**, 2019, 2600–2606.
11. STAN, F., STANCIU, N.-V., SANDU, I.-L., FETECĂU, C., ȘERBAN, A., Effect of low and extreme-low temperature on mechanical properties of 3D- printed polyethylene terephthalate glycol, *Ro. J. Techn. Sci. - Appl. Mechanics*, **64** (1), 2019, 21-41.

Manuscript received: 21.10.2020